VILNIUS TECH
Vilnius Gediminas Technical University

TRANSPORT

Original Article

APPLYING REGULAR RELIEF ONTO CONICAL SURFACES OF CONTINUOUSLY VARIABLE TRANSMISSION TO ENHANCE ITS WEAR RESISTANCE

Volodymyr DZYURA[1], Pavlo MARUSCHAK[2✉], Stoyan SLAVOV[3], Diyan DIMITROV[4]

[1,2]*Dept of Wheel Vehicles, Ternopil Ivan Puluj National Technical University, Ukraine*
[3]*Dept of Manufacturing Technologies and Machine Tools, Technical University of Varna, Bulgaria*
[4]*Dept of Mechanics and Machine Elements, Technical University of Varna, Bulgaria*

Highlights:

■ the causes of surface defects formed on the working surfaces of the conical discs of stepless transmissions are systematized and classified;
■ the relationship between the process parameters and service characteristics of the working surfaces of the conical discs making part of the variator transmissions of vehicles is established;
■ a RMR is proposed to be formed on the working surfaces of the conical discs of stepless transmissions to improve their service characteristics;
■ dependencies are established between the conditions, under which a partially RMR is formed (strain forces and feedrate), and microgeometric quality parameters;
■ the tool trajectory of a deforming element was obtained using a new approach based on the so-called "Commis–Voyageur problem" algorithms, which allowed us to consider using these methods for generating the tool trajectory.

Abstract. While investigating the variator transmission of vehicles, the relationship between the technological and service parameters of the working surfaces of conical disks treated by technological methods was established. The service properties are proposed to be enhanced by Regular MicroReliefs (RMRs) created on such surfaces. The optimal technological processing conditions were found, which allow retaining the greatest amount of lubricant. The causes of surface defects, formed on the working surfaces of conical disks of the Continuously Variable Transmission (CVT), are systematized and classified. The wear resistance of such surfaces is proposed to be enhanced by technological methods, in particular, by forming partially RMRs on them. Their application facilitates relaxation processes on the material near to the surface, reduces shear stresses and strains, thus preventing the formation of burrs and extending the life of the conical disks of the CVT. A novel approach for obtaining the tool-paths of the deforming element, based on the so-called "Commis–Voyageur problem" algorithms, is employed in order to research the possibilities for involving that methods in toolpath generation. Dependences between the partial RMR's formation conditions (deforming forces and feedrate) and microgeometric quality parameters are established. The latter include surface roughness, with a partially RMR applied onto the face surfaces of the test specimen (rotary body). It is found that these microreliefs enhance the ability of oil retaining in plastically deformed traces, formed over the operational surfaces, in comparison with those, that are processed by traditional cutting methods, as turning for example.

Notations

ANOVA – analysis of variance;
CAD – computer-aided design;
CAM – computer-aided manufacturing;
CNC – computer numerical control;
CVT – continuously variable transmission;
DXF – drawing exchange format;
NC – numerical control;
RMR – regular microrelief;
TSP – travelling salesman problem;
VIF – variance inflation factor.

Introduction

A CVT provides in the torque transmission and smooth gear a certain range (Van der Meulen 2010; Seigars 2016). The variable transmissions have a fairly simple design. The main component of which is a metal belt that rotates between 2 cones, installed with vertices, facing each other. The automatic shift of the belt from the top of the cone to its base and vice versa changes the gear ratio and, accordingly, the speed of the vehicle. The disadvantage of such transmissions is a rather short life, while its advantages include low torque transmission losses, continuous speed control and, accordingly, high fuel efficiency.

CVTs are very common in JF011E variators applied in the following vehicles *Dodge Caliber*, *Nissan X-trail*, *Nissan Qashqai*, *Nissan Teana*, *Nissan Tiida*, *Mitsubishi Lancer*, *Mitsubishi Outlander*, *Mitsubishi Galant*, *Mitsubishi GalantASX*, *Peugeot 4007*, *Renault S7*, *Renault Fluence*, *Renault Koleos* another one denoted as JF015E variators are used in *Nissan Juke*, *Nissan Micra*, and *Suzuki Swift* cars. It is noteworthy that the heat losses, suffered by variators are greater than in the case of typical gearboxes. A high heat loading reduces the service life of oil and the variator itself, which does not normally exceed 100000 km. Therefore, an additional cooling area for the variator discs is an important technological task. One of the solutions is applying a RMR onto the surfaces of the variator disks. In addition, the process parameters of forming partially RMRs need to be substantiated in order to ensure a guaranteed oil wedge on the friction surface. The relief improves friction and wear conditions (Pawlus *et al.* 2019; Nanbu *et al.* 2008; Zajdes, Hin 2017). However, the technology for applying a RMR onto parts of different geometries requires further development with focus on ensuring optimal roughness, surface hardness, and minimizing the friction coefficient (Nagît *et al.* 2019; Swirad, Pawlus 2021).

Shnejder & Lebedinskij (1970) have found that a RMR of the 1st type with a relative area of 35% is the best solution for metal parts that perform a relative movement in terms of service period, lifetime duration and oil film thickness and its size.

Other authors investigated how the shape of the microrelief may affect the size of the contact area with the liquid (Bulatov *et al.* 1997), the set of concave cones, spherical holes and longitudinal lines. The microrelief, featuring a set of conical holes, was proved to be the most optimal, with the other parameters being identical. An important aspect is the influence of the microrelief on the friction coefficient (Wos *et al.* 2020). The lowest friction coefficient was obtained during the interaction between end surfaces of rotary bodies, onto which we applied the RMR with a central microroughness angle of 90° oriented towards the outer sides of the end surface (Wos *et al.* 2020).

There are articles, dedicated to technological issues (Slavov, Dimitrov 2018; Kiselev *et al.* 2009; Sánchez Egea *et al.* 2019). They show a project of the *L8 Taguchi tool* to form a RMR on planar surfaces. The influence parameters, affecting the formation process of RMR, using a CNC milling machine on flat surfaces, were determined. RMRs of different sizes and groove arrangement patterns were formed. The results obtained are a prerequisite for optimizing the conditions of forming RMRs.

The influence of the deforming force with respect to permanent deformation occurrence and feedrate on the surface roughness parameters during burnishing are investigated by Sánchez Egea *et al.* (2019) along with mechanical properties of the surface layer. In addition, parameters of the surfaces obtained by ball-burnishing are compared. The optimal pressure range during ball-burnishing of specimens, at which roughness parameters were the lowest, was found. Certain issues, relating to the relationship between quality parameters and performance of the working surfaces of the end surfaces of rotary bodies, are considered by Nagorkin *et al.* (2017, 2018) and Costa & Hutchings (2015).

The possibilities for improving the CVT by minimizing the variator's clamping forces are described in research by Bonsen *et al.* (2005). To this end, the slip control technology is used. This approach provides for the best possible transmission efficacy combined with the increased resistance to slippage damage. The authors describe the relationship between the slippage of the variator belt and the functional properties of the transmission. The optimal performance conditions in terms of strength and efficiency are determined. The experimental investigations conducted suggest that the clamping force of the belt must be reduced to very low values in order to enhance the efficiency in low torque conditions. At the same time, the problem of finding the optimal clamping force under low load conditions while maintaining a quick hydraulic response remains unsolved.

Findings with regard to the clamping force are also presented in research by Bonsen *et al.* (2004). The benefits resulting from efficacy were found to be lost due to the CVT's inefficiency, in particular, due to losses that occur mainly in the (hydraulic) drive system and in the variator. Such losses can be reduced by minimizing the clamping force of the belt's pulleys. However, when reduced to very low values, clamping forces bring about the excessive belt-to-pulley slippage, causing damage to the system. By controlling the clamping force in such a way as to allow for a limited slippage, the clamping force can be minimized without risking damage to the system, the cone discs and the drive belt itself. To control slippage, a non-linear control scheme is used in the variator. This method was shown to be robust to torque peaks.

Findings by Yagyaev *et al.* (2020) with regard to reliability of the car variator are the closest to the problem considered. According to the authors, the variator's performance is ensured by the surface layer's quality, manufacturing accuracy, and surface microrelief of the pulley and steel wedge belt. The pulley processing technique is crucial when it comes to ensuring the variator's reliability. RMRs were proposed to be created on the finished pulley

surface by laser ablation, which acts as microchannels to improve oil drainage from the contact structure. Oil channels created on the pulley surface by laser ablation are well located and allow obtaining the required pattern, direction, depth and length.

Regardless of the fact that variable transmissions have already occupied a certain niche in car making, enhancing their reliability and manufacturability to extend their service life is an important task. There are a number of efforts for analysing the height-related roughness parameter R_a (Wang *et al.* 2010; Volchok *et al.* 2002; Dzyura *et al.* 2021a, 2021b, 2021c). The service characteristics of surfaces, in particular, the ability to retain oil, were investigated, using the group of R_k parameters on the Abbott–Firestone diagram, based on surface profilograms of test specimens. Comparative studies of the ability to retain oil by surfaces, formed by different technological operations with different microgeometric quality parameters, were conducted.

However, the effect of the conditions, under which the partially RMR is formed, such as feed and deforming forces, as well as the geometric microrelief parameters, such as the axial step of roughness, requires further study. From a practical point of view, it is important to determine the relationship between the process parameters, which can be controlled, and the working surface quality of machine parts, as well as their performance characteristics, because they greatly affect the life of these parts and components in general. In addition, taking into account the current trends in creating methods and algorithms for (self-) optimization in industrial systems, represented in the concept of *Industry 4.0*, it is important to develop and research some new approaches for generation of the needed toolpaths (with optimal length and shape) for RMR formation, based on predefined characteristic points (i.e., "nodes").

Therefore, the main goals of the current research are: on 1st place, to identify the effect of the conditions for the RMR forming at geometric characteristics and oil retaining. The sub-aim was focused on the process for tool paths at an optimal length with respect to the ball-burnishing method, based on some of the existing for solving the so-called "Commis–Voyageur problem" (TSP).

1. Materials and methods

The studies, described in the article, were conducted in 2 stages:

- at the 1st stage, the variator disc of the Nissan Juke car, manufactured by *Jutco*, which was made of steel 17G1S (C = 0.15...0.20; Si = 0.4...0.6; Mn = 1.15...1.6; Ni ≤ 0.3; S ≤ 0.04; P ≤ 0.035; Cr ≤ 0.035; Cu < 0.3) and had a mileage of 93 thousand km, was investigated. The axial section of the disk was trapezoidal. The fractographic features of the metal of the working surfaces were studied, taking into account the service resources. Therefore, the fractographic features of damage in different parts of the disk were analysed. For this case an EVO-40XVP scanning electron microscope was used;

- at the 2nd stage, a new approach was used to enhance the ability of the contact surfaces of the disc to retain lubricant substances by forming partially RMR, using ball-burnishing process. The required toolpaths were elaborated by a novel algorithm, shown in Figure 1. As input parameters it uses X and Y coordinates of the toolpath characteristic points, calculated by the methodology (Dzyura *et al.* 2021a, 2021b, 2021c). Factors are selected according to expert assessments and based on the analysis of scientific literature (Swirad, Pawlus 2021; Shnejder, Lebedinskij 1970; Bulatov *et al.* 1997; Wos *et al.* 2020). Int the 1st step (Step 1 from Figure 1), the calculated points coordinates were formatted into 3-column matrix and exported as *.tsp* file, in order to be readable by *Concorde TSP Solver* (*https://www.math.uwaterloo.ca/tsp/concorde.html*, Applegate *et al.* 2002). Int the 2nd step (see Step 2 from Figure 1), the toolpaths points were considered as nodes from the integrated in *Concorde TSP Solver* algorithms, in order to find an optimal route through them (Figure 2a). As a result, from Step 2, a reordered set of the points coordinates was obtained, which assures the minimum length of the toolpath. In Step 3 of the algorithm from the optimally ordered points, a continuous polyline was created and exported as DXF file. Then the DXF file was imported into the CAD–CAM software (in our case *Solidworks*, *Dassault Systèmes*) and the polyline is used by the *Solidworks'* CAM module as an entity for the trajectory, defining the ball-burnishing operation (Step 4 on Figure 1). These steps repeated, until the last' segment of the RMR was processed.

When all RMRs are formed in this way, the corresponding NC-code is generated by the *Solidworks'* CAM module.

The effects of some of the ball-burnishing regime parameters and ball tool trajectories, under which partial RMRs are proposed, at heights of surface roughness, using R_a criterion (according to GOST R ISO 4287-2014). In this regard:

- the effect of the axial pitch of grooves on the surface roughness at different RMR formation conditions was evaluated;

- the effect of RMR formation conditions on the geometrical characteristics of surfaces was studied.

The conical drive elements of variators can be considered as disks. As test specimen a disk made of 17G1S steel (with a diameter of 180 mm and thickness of 15 mm) was prepared by turning, shown on Figure 2b. The initial surface roughness of the surfaces of the specimen faces was $R_a \approx 16$ μm achieved after finish turning operations. The values of the main ball-burnishing regime parameters that were used in the current experiments were summarized in Table 1. Classification of the main causes of failure of variable transmission of cars can be seen in Table 2. Values, which presented in Table 3, are corresponding to the full factorial experimental design where each factor is varied at 3 levels: low, middle and high. The full experimental design with natural values of the participated factors can be seen in Table 3.
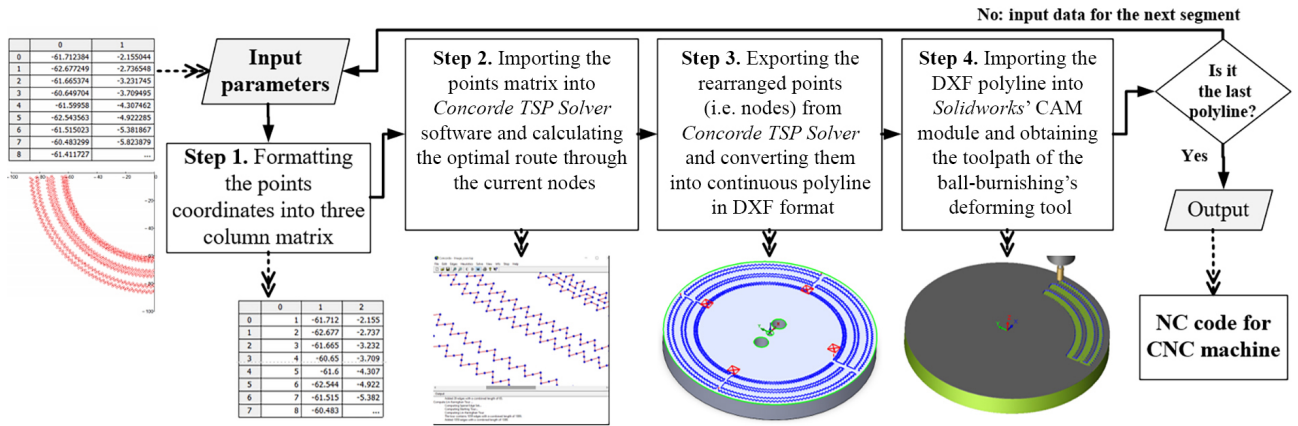
Figure 1. An algorithm for generating optimal toolpaths for ball-burnishing operation, based on the methods for solving TSP

Table 1. Variation levels of the ball-burnishing process' regime and toolpaths parameters for research the roughness characteristics of the surface with partially RMR, formed onto faces of disk

Processing modes	Denotation	Numerical values of processing modes		
Deforming force [N]	$F_{d.i}$	600	400	200
Feedrate [mm/min]	$f_{in.i}$	1500	1000	500
Distance between the axes of the grooves (Figure 2a) [mm]	S_o	4	3	2

Table 2. Classification of the main causes of failure of variable transmission of cars

Damage type[*]	Causes	Reparability [+/–]
1. Disk damage	–	–
1.1. Wear: ■ local violation; ■ distortion of the cone shape	Local actuation of cone's geometry, caused by belt slippage in local areas (punching)	–
1.2. Burrs, grooves, scratches: ■ burrs; ■ grooves; ■ scratches	Local defects, caused by solid particles or insufficient lubrication	Grinding is possible in case of minor damage only
1.3. Corrosion	Local corrosion damage, caused, for instance, by storage conditions	Grinding is possible in case of minor damage only
1.4. Deformation of disks: ■ mechanical; ■ thermomechanical	As an effect of overloading, local force and/or temperature, stresses and strains	–
2. Damage to the high-pressure pump	Wear of the bypass valve, pressure drop in the system, as a result of which there is a slippage of a belt and additional wear of cones	Bypass valve replacement
3. Damage to the high-pressure pump	Wear of the bypass valve, pressure drop in the system resulting in the belt slippage and additional wear of the conical surface.	Bypass valve replacement
4. Damage to the belt: ■ burrs; ■ abrasion due to slipping	Connected with overloading, stress gradient, dry friction conditions	–

Note: [*] damage, for the prevention of which technological measures have been developed, is pasted "grey" colour.

The shape and dimensions of the tested specimen were selected in order the formed RMR segments to be located optimally onto their face's areas. Both of their face surfaces were divided into nine sections (segments), Figure 2. In this way, the described specimen could be used for all of the 27 trials (Table 3), according to the experimental design.

The other ball-burnishing process parameters had fixed values during all of the trials: diameter of the ball tool was equal to 6 mm, *Mobil* DTE 25 hydraulic oil was used as a lubricant. All of the partially RMRs were processed, using HAAS TM-1 CNC milling machine, and specially designed tool for ball-burnishing (Figure 2b) (Slavov, Iliev 2016).

Table 3. Values of the roughness parameter and variable parameters in experimental studies

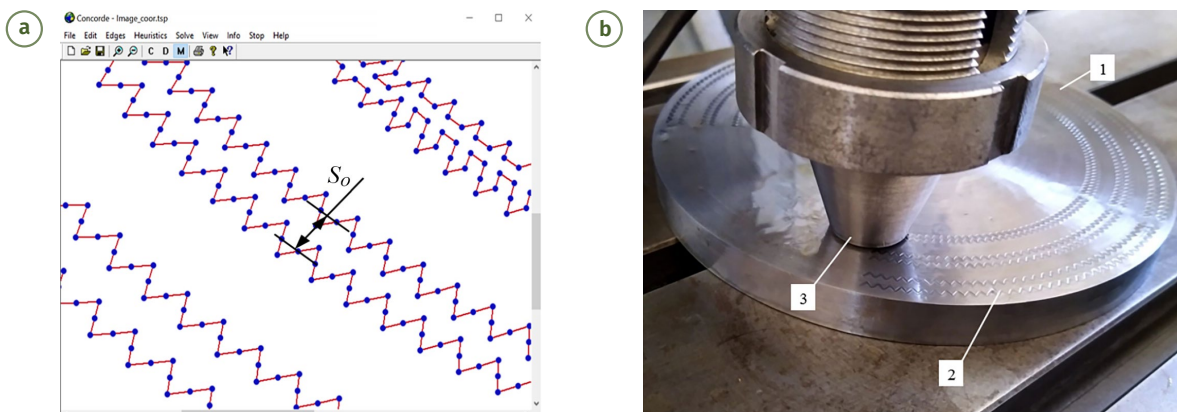| Experiment number	Section	Area	Axial pitch of the grooves $S_{o,i}$ [mm]	Deforming force $F_{d,i}$ [N]	Feedrate $f_{in,i}$ [mm/min]	Measured values of the roughness criterion R_a [µm]	Fitted by using Equation (1) values of R_a [µm]
1		1	2	200	500	1.11	1.57
2	1	2	3	200	500	1.37	2.29
3		3	4	200	500	3.05	3.01
4		1	2	400	500	5.98	5.48
5	2	2	3	400	500	7.37	6.20
6		3	4	400	500	7.40	6.92
7		1	2	600	500	7.40	9.38
8	3	2	3	600	500	11.99	10.12
9		3	4	600	500	10.16	10.82
10		1	2	200	1000	2.74	1.88
11	4	2	3	200	1000	2.80	2.60
12		3	4	200	1000	3.11	3.32
13		1	2	400	1000	5.69	5.78
14	5	2	3	400	1000	7.78	6.50
15		3	4	400	1000	8.13	7.22
16		1	2	600	1000	8.17	9.69
17	6	2	3	600	1000	8.62	10.41
18		3	4	600	1000	11.36	11.13
19		1	2	200	1500	1.81	2.18
20	7	2	3	200	1500	1.45	2.90
21		3	4	200	1500	1.45	3.62
22		1	2	400	1500	8.26	6.09
23	8	2	3	400	1500	7.31	6.81
24		3	4	400	1500	9.57	7.53
25		1	2	600	1500	10.64	9.99
26	9	2	3	600	1500	10.31	10.71
27		3	4	600	1500	10.53	11.43

Figure 2. Optimal length toolpaths generation and their realisation for obtaining partial RMRs onto conical surfaces: (a) – resultant tours from *Concorde TSP Solver*; (b) – forming RMRs with 3 different axial steps on the tested specimen's surface (1 – tested disk; 2 – segments with RMR; 3 – front end of the device for processing RMRs)

The surface roughness was measured using surface roughness tester – *Mitutoyo, SurfTest* SJ-301. This device generates surface roughness certificates that include graphical representations of the roughness profile and automatically calculates the roughness height criterions R_a, R_q and R_z.

The cut-off length of the currently measured traces was selected to be 2.5 mm, in order to capture the several toolpath segments. The roughness measurements methodology is described in detail by Volchok *et al.* (2002).

2. Fractodiagnostics of CVT

The general view of the CVT with conical working surfaces was analysed, Figure 3 (Van der Meulen 2010). The principle of its operation is as follows: a metal belt 1, which consists of typesetting metal plates, rotates the Slave pair of cones 2, being stretched between them. The conical disks of the transmission are coaxial, with smaller diameters, facing each other. The gear ratio changes smoothly due to the displacement of the cones, relative to each other and, accordingly, the movement of the belt either to the "narrow" or "wide" parts of the cones. At the same time, a similar pair is located on the Master part of the transmission, which works synchronously, however, in antiphase (when the Master cones converge, the Slave cones diverge). This provides for the belt tension and a smooth change in gear ratio. The torque, transmitted by such variators, varies in the range of 140...170 N·m.

The advantages of such component include:
- smooth, continuous switching;
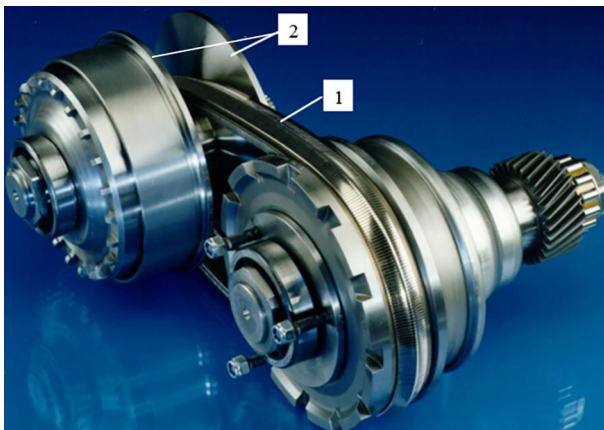- cost-efficiency;
- noiseless operation;
- fast actuation.

Figure 3. General view of CVT (Van der Meulen 2010):
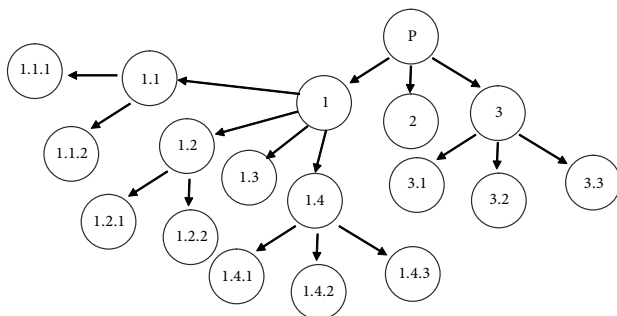1 – belt; 2 – conical discs

Figure 4. Causes of variator failure:
1 – damaged discs; 1.1 – wear; 1.1.1 – local violations of geometry; 1.1.2 – distortion of the cone shape; 1.2 – burrs, grooves, scratches; 1.2.1 – burrs; 1.2.2 – grooves, scratches; 1.3 – corrosion; 1.4 – disk permanent deformation; 1.4.1 – mechanical damage; 1.4.2 – thermomechanical damage; 2 – damage to the high pressure pump; 3 – damage to the belt; 3.1 – burrs; 3.2 – abrasion due to slipping

Its disadvantages include:
- restrictions on use on powerful cars;
- sensitivity to uneven movements, abrupt starts, low road conditions, slipping.

Therefore, the variable type of transmission is not designed for rigid driving style, which may cause its damage, overheating, abrasion of disc surfaces, wear and other types of damage, the structure of which proposed by the authors in Figure 4.

The damaged working surface of the CVT conical disk was investigated by the methods of macro- and microanalysis, Figure 5. A photo of in-service defects of the working surfaces of CVT conical disks was obtained. As it is seen, the disk surface is covered with circular scratches (A) caused by shifting and setting of the material in these areas. Circular scratches border on less damaged areas of abrasions (B), indicating the localization of the disk wear in certain areas (Dzyura *et al.* 2021a, 2021b, 2021c).

Within individual scratches, one can notice traces of slipping and micro-eruptions in the direction of slipping. However, no specific surface layers with a structure different from that of the steel disk were found.

With significant magnifications, scanning electron microscopy revealed micro-tears-out (C), which occurred due to the contact of the disk material and that of the metal belt (Figure 6a). They have a connected with overloading texture and indicate on a high value of stress comparing to mechanical parameters of the material used (Guzanová *et al.* 2015). In addition, shear micro-flanges (D) were
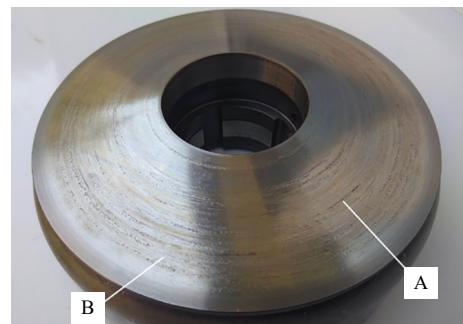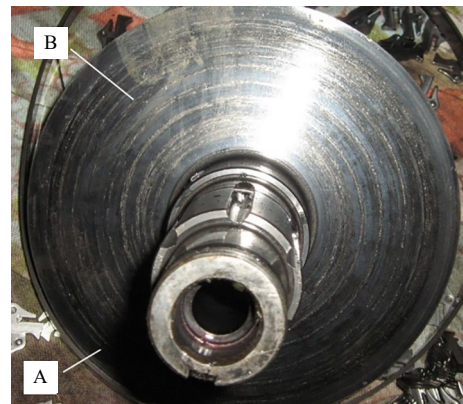

Figure 5. Working surface of the CVT conical disk with damages in a form: A – circular scratches; B – areas of abrasions
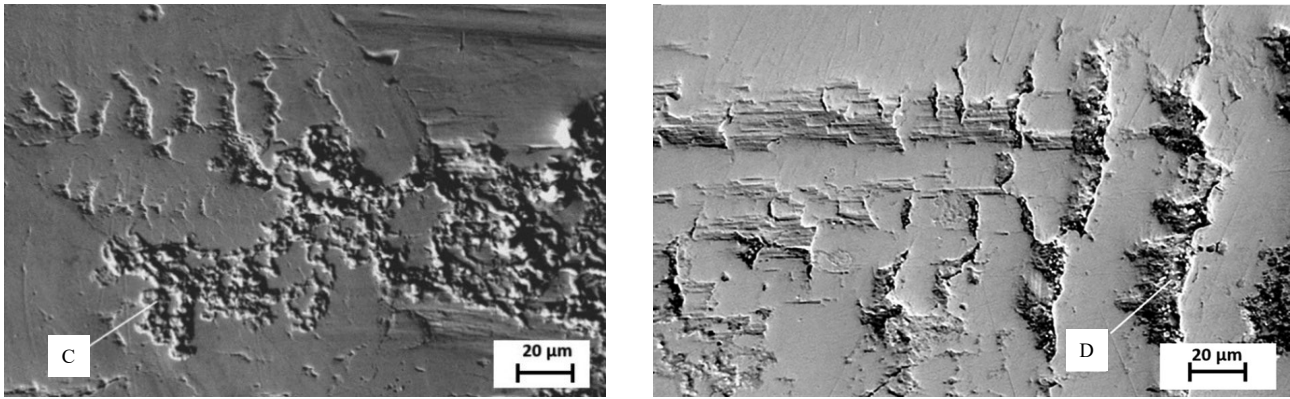
Figure 6. Images of in-service micro-defects of working surfaces of CVT conical disks, obtained by means of scanning electron microscopy: C – micro-tears-out; D – shear micro-flanges

found on the surface, indicating slippage at a significant plastic deformation at the micro level (Figure 6b).

These micro-defects can be of 2 subtypes:

- micro-chipping in the form of pits, caused by local strains and possibly the material fatigue under overheating conditions, with a sudden slippage of the belt, relative to the disk surface with a sharp change in torque;
- micro-flanges, caused by the slipping of the belt on the disk metal in the absence of integrity of the oil film or by virtue of its impairment, as well as due to the abrasive action of microparticles, exfoliated from the surface.

3. Analysis of the experimentally obtained results for the regime parameters influence over of the surface roughness R_a criterion

The experimental results are subjected of the regression analysis methodology using the specialized statistical software Minitab (*https://www.minitab.com/en-us/products/minitab/*). The results obtained for R_a roughness criterion are shown in the Table 3 for each of the 27 trials within the experimental study design. In the 1st step of the analysis only main factors was taking into account as regression terms. Using them, the coefficients of a regression equation was derived at α = 95% confidence level. They are shown in the Table 4, along with their statistical assessment criterions.

As can be seen from Table 4, the Student's criterion (i.e., T-value) of the coefficient in front of the regime parameter – feedrate f_{in} has the lowest value, and it falls outside from the allowable confidence interval. As result, its P-value exceeds significantly the maximum allowable level of 5% probability to reject wrongly the Null hypothesis, which states that the coefficient in front of the "feedrate" term is insignificant. Therefore, the regime parameter feedrate could be considered as insignificantly influencing over the roughness height criterion R_a, and as result could be excluded from the regression equation. The VIFs of the calculated predictors are equal to 1.0 (Table 4), which means

that they are not correlated each other. Considering those, the regression equation take the following form:

$$R_a \text{ [μm]} = -4.08 + 0.01952 \cdot F_d \text{ [N]} + 0.720 \cdot S_o \text{ [mm]},\qquad(1)$$

where: R_a – roughness criterion; F_d – deforming force; S_o – distance between the axes of the grooves.

The R_a values calculated by using the regression equation are shown in the last column of the Table 3 for comparison. The R-square (i.e., R^2) value, calculated for the regression equation is equal to 88.47%. Therefore, it can be consider that there is comparatively good fit between values calculated by the regression equation and experimentally obtained values for the roughness height's criterion R_a.

In order to confirm the derived above results for the terms' significance of the regression, an ANOVA also has been carried out, the results of which are shown in the Table 5.

The results from the carried out ANOVA analysis (Table 5) confirms the significance of the terms that participate in the regression equation, based on the Fisher statistics (F-value). It can be seen from Table 5 that the Fishers statistics (F-value) of the regime parameter feedrate f_{in} has the lowest value again, and the same result for the P-value, as those calculated in the Table 4. The other 2 regime parameters from the regression equation – deforming force and distance between the axes of the adjacent grooves, can be considered as statistically significant based, on their F-values and P-values.

The contribution degrees of each of the regression terms are calculated (Table 5). As can be seen the deforming force causes 85.06% of the impact over the roughness' height criterion R_a, while the other 2 regime parameters have common contribution lesser than 3.5%. Pareto diagram of the standardized effects of the regime parameters, along with 2 residual plots are shown in the Figure 7a –c, in order to confirm the adequacy of the derived regression equation.

Table 4. Regression's coefficients of main terms and their statistical assessment

Term	Regression coefficient	Standard error	Confidence interval at 95%	*T*-value	*P*-value	VIF
Constant	−4.08	1.26	(−6.69; −1.47)	−3.24	0.004	–
f_{in} [mm/min]	0.000611	0.000600	(−0.000629; 0.001851)	1.02	0.319	1.00
F_d [N]	0.01952	0.00150	(0.01642; 0.02263)	13.03	0.000	1.00
S_o [mm]	0.720	0.300	(0.100; 1.340)	2.40	0.025	1.00

Table 5. Results for the terms' significance participated in the regression equation, based on ANOVA analysis carried out

Source	Degrees of freedom	Sequential sum of squares	Contribution	Adjusted sum of squares	Adjusted mean square	*F*-value	*P*-value
Regression	3	285.494	88.47%	285.494	95.165	58.82	0.000
f_{in} [mm/min]	1	1.681	0.52%	1.681	1.681	1.04	0.319
F_d [N]	1	274.482	85.06%	274.482	274.482	169.66	0.000
S_o [mm]	1	9.331	2.89%	9.331	9.331	5.77	0.025
Error	23	37.210	11.53%	37.210	1.618	–	–
Total	26	322.705	100.00%	–	–	–	–

The Pareto chart shows the ranking of factors by degree of influence based on calculated standardized effect. As can be seen from Figure 7a the standardized effects of the factors: deforming force F_d, and distance between the axes of the adjacent grooves So, exceeds the reference level of 2.07, determined for the current regression model parameters, while the feedrate is below of that level, and therefore could be neglected. The normal probability plot of the residuals displays the residuals versus their expected values. If the distribution is normal that plot should approximately follow a straight line. If the residuals do not follow a normal distribution, the confidence intervals and p-values can be inaccurate. As can be seen from the Figure 7b, the normal probability plot of the residuals, derived for the regression equation, have located close enough to the line, which is indication of the normal distribution. The residuals versus fits plot (Figure 7c) is used to verify the assumption that the residuals are randomly distributed and therefore have constant variance. Theoretically, the points should fall randomly on both sides of the zero line, with no recognizable patterns in the points. As can be seen from the Figure 7, there is no distinguished pattern in the residuals distribution, which allows concluding that the regression equation has constant variance.

On the 2nd step of the analysis 2-way interactions between the regime parameters was included in the regression equation. The significance of the regression's terms with them was assessed again using ANOVA, and the obtained results are shown in the Table 6.

As can be seen from Table 6, the 2-way interactions increase the overall contribution of the regression model in comparison with the regression from the 1st step, but their common contribution is not substantial (less than 5%). At the same time, statistical evaluations based on Fisher statistics (*F*-value) of the 2-way interactions shows that the null hypothesis cannot be rejected for them. Therefore, the 2-way interactions in the regression are considered as statistically insignificant, and could be neglected in order to avoid the model unnecessary complication.
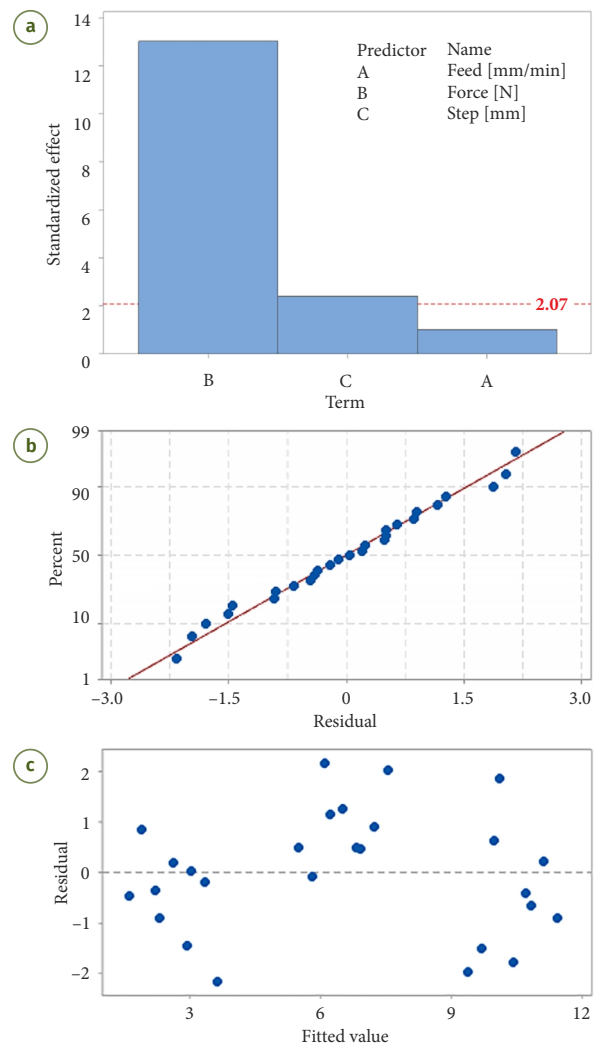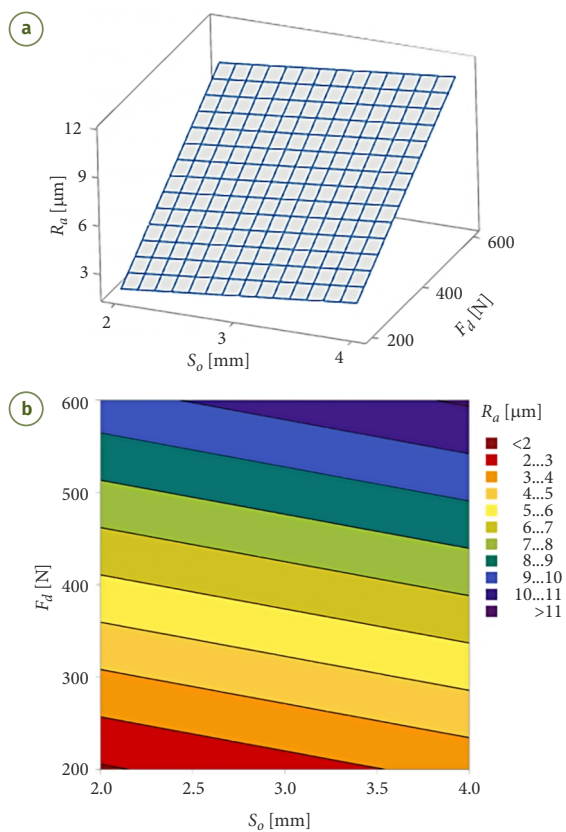
Figure 7. Graphical representation of the regression model statistical assessments:
(a) – Pareto chart of the standardized effects of the regime parameters from the regression equation (response is R_a [μm]; α = 0.05); (b) – normal probability plot of residuals; (c) – residuals versus fits graph of the regression

Table 6. ANOVA analysis of the regression with 2-way interactions included

Source	Degrees of freedom	Sequential sum of squares	Contribution	Adjusted sum of squares	Adjusted mean square	F-value	P-value
Regression	18	314.182	97.36%	314.182	17.455	16.38	0.000
Linear	6	298.945	92.64%	298.945	49.824	46.77	0.000
f_{in} [mm/min]	2	1.683	0.52%	1.683	0.841	0.79	0.486
F_d [N]	2	287.893	89.21%	287.893	143.946	135.12	0.000
S_o [mm]	2	9.370	2.90%	9.370	4.685	4.40	0.051
2-way interactions	12	15.237	4.72%	15.237	1.270	1.19	0.413
f_{in} [mm/min] · F_d [N]	4	6.676	2.07%	6.676	1.669	1.57	0.273
f_{in} [mm/min] · S_o [mm]	4	6.216	1.93%	6.216	1.554	1.46	0.300
F_d [N] · S_o [mm]	4	2.345	0.73%	2.345	0.586	0.55	0.705
Error	8	8.522	2.64%	8.522	1.065	–	–
Total	26	322.705	100.00%	–	–	–	–

Figure 8. Graphical representation of the response surface obtained by the regression equation: (a) – surface plot of R_a [μm] vs F_d [N], S_o [mm] from regression equation; (b) – contour plot of R_a [μm] vs F_d [N], S_o [mm] from regression equation

As result, the impact of the ball-burnishing process' regime parameters on the R_a roughness criterion is assessed using the linear regression equation. In the Figure 8a–b contour and surface plots are shown, obtained for the middle value of the feedrate f_{in} =1000 mm/min as illustration of the manner of the influence of the statistically significant regime parameters.

Since the traditional finishing operations (turning, grinding), which are used to extend the disc life, do not enhance its durability, recommendations to apply regular relief onto such surfaces were given. In contrast to the above-mentioned methods that create a chaotic micro-relief characterized by sufficiently sharp peaks of micro-irregularities and low ability to retain oil, the partially RMR provides for a high manufacturability of surfaces. When the partially RMR was formed on the test specimen surface (Figure 2b) (Dzyura et al. 2021a, 2021b, 2021c), the surface roughness increased slightly.
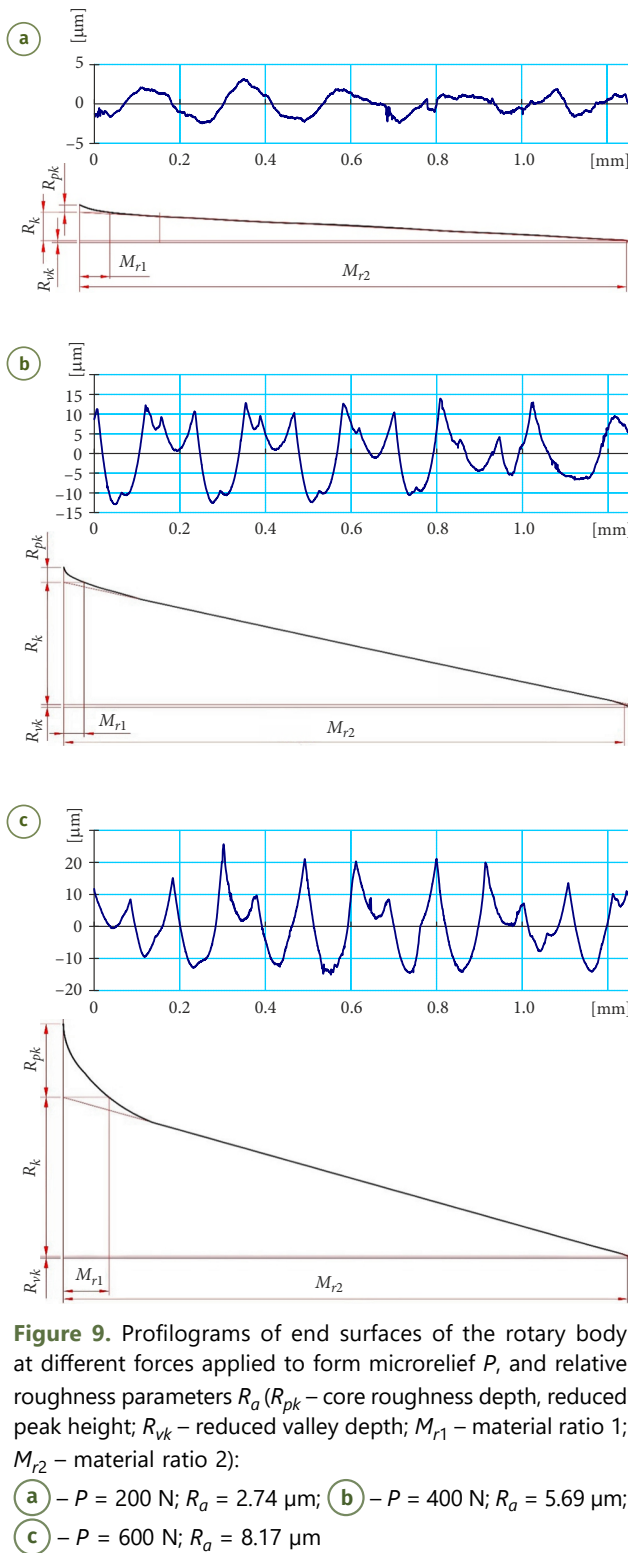
4. Discussion

4.1. The algorithm for generating optimal tool paths to ball-burnishing operation

The created algorithm (Figure 1) gives opportunity for obtaining tool trajectories at permanent deformation with the shortest overall length. The optimal length of the path is reached on the base of the approaches for solving TSP, included in *Concorde TSP Solver* software tool. In the current investigation, the best results for RMR's toolpath generation was obtained when Kernighan–Lin heuristic algorithm was used (Helsgaun 2000). The parameters of the K–L algorithm were as follows: the number of kicks used per iteration was 40 and close for the type of the kick was chosen. As it can be seen in Figure 2a, when the distance between the adjacent grooves has larger values (S_o is equal to 3 and 4 mm), the algorithm generates correct routes between the trajectory nodes. However, when S_o is 2 mm, the resulting route does not pass through the nodes properly, due to the equality of the distances between them in the different directions. Therefore, in those cases, the number of the toolpath's nodes along the desirable trajectory should be increased, in order to control the right route tracing.

4.2. The surface roughness profilograms

Operational characteristics of the surfaces with RMR applied onto them were evaluated according to the Abbott–Firestone curves. The characteristics of their profile were established according to the R_k parameter (Dzyura

Figure 9. Profilograms of end surfaces of the rotary body at different forces applied to form microrelief P, and relative roughness parameters R_a (R_{pk} – core roughness depth, reduced peak height; R_{vk} – reduced valley depth; M_{r1} – material ratio 1; M_{r2} – material ratio 2):

(a) – P = 200 N; R_a = 2.74 μm; (b) – P = 400 N; R_a = 5.69 μm;
(c) – P = 600 N; R_a = 8.17 μm

et al. 2021a, 2021b, 2021c). The ratio of the material filling length to the estimated cut length (%) was calculated. The slope at the beginning of the curve reflects the profile peaks, which were important during the run-in period. The slope at the end of the curve reflects the depressions of the microrelief profile, which were the reservoirs of lubricant. The relief was found to have signs of orderliness for the cases considered, which is noticeable from the profilograms shown on Figure 9.

Standard ISO 21920-2:2021 provides a dependency for determining the amount of oil that will be retained on the surface:

$$V_o = \frac{R_{vk} \cdot (100 - M_{r2})}{200}, \tag{2}$$

where V_o is the capacity that contains lubricant [mm³/cm²] (the amount of oil that can be retained on the surface of the investigated disk is calculated according to the values obtained from the diagram (Table 7)); M_{r2} – material ratio 2.

The surface with the partially RMR applied onto it (roughness parameter R_a = 5.69 μm) is optimal in terms of the amount of oil retained, as evidenced by the analysis of Abbott–Firestone curves (Dzyura et al. 2021a, 2021b, 2021c). This value of the roughness parameter was obtained under the following conditions: $F_{d.i}$ =400 N; $f_{in.i}$ =1000 mm/min. Taking into account the optimal value of the deforming force, these results correlate well with those presented by Nagît et al. 2019).

An increase in the deforming force $F_{d.i}$ from 400 to 600 N leads to a significant increase in the surface roughness parameter R_a from 5.69 to 8.17 μm, as well as to a significant decrease in the surface ability to retain oil, Table 4. In addition, an increase in the feedrate from 500 to 1500 mm/min also leads to an increase in surface roughness by an average of 3 μm and can be considered as a way to significantly increase the productivity of applying RMRs on such surfaces.

However, from the perspective of wear intensity, which is estimated by the R_k parameter, the surface with R_a = 2.74 μm obtained at the deforming force $F_{d.i}$ = 400 N is optimal.

The regular relief, applied onto CVT discs, the technological bases of which are described in this article, improves the tribological characteristics of CVT discs. In addition to having oil accumulated in depressions, the microrelief's profile promotes relaxation processes on the surface, reduces values of shear stress and strain, thus preventing the formation of burrs (Dzyura, Maruschak 2021).

Table 7. Parameter values for determining service characteristics of surfaces with a partially RMR applied onto them

No	Deforming force $F_{d.i}$ [N]	Roughness parameter R_a [μm]	Parameters of the R_k group of the Abbott–Firestone curve		The amount of oil retention V_o [mm³/cm²]
			R_{vk}	M_{r2}	
1	200	2.74	0.2856	99.080	0.001314
2	400	5.69	0.5304	98.810	0.003156
3	600	8.17	0.3332	99.430	0.000949

Conclusions

The reasons for damage occurrence on CVT disks were estimated by SEM approach. In particular, numerous scratches and surface tears-out were observed at the macro level, while individual micro-chipping and micro-flanges occurred at the micro level. These macro- and micro-defects were found to result from the slipping of the belt on the disk metal in the absence of integrity of the oil film or by virtue of its impairment, as well as due to the abrasive action of microparticles, exfoliated from the surface, which caused its local overheating and wear. This requires the development of technology that would ensure a guaranteed ability of the surface of the variator disc to retain oil.

The ball-burnishing process regime parameters were substantiated. These parameters were used to forming partially RMRs that provide for a guaranteed oil layer on the friction surface. The quality of the working surfaces of the test specimen, previously subjected to the finishing turning operation, were evaluated in quantitative terms according to the Abbott–Firestone curve.

The used approach for toolpath generation with optimal length, based on the TSP's heuristic algorithms, demonstrates promising enough results. Although some drawbacks are encountered in some particular distributions of the nodes, the used approach for toolpath generation with optimal length, based on the TSP heuristic algorithms, gives acceptable results. Therefore, the approach could be used as a base for developing algorithms that are more appropriate for toolpath generation in future, especially when the toolpath must have a more complex shape. Thus, the research findings will be of significant practical importance in those areas where they extend the service life of variator transmissions of vehicles with continuously variable speed control.

Acknowledgements

References

Applegate, D.; Cook, W.; Dash, S.; Rohe, A. 2002. Solution of a min-max vehicle routing problem, *INFORMS Journal on Computing* 14(2): 132–143. https://doi.org/10.1287/ijoc.14.2.132.118

Bonsen, B.; De Metsenaere, C; Klaassen, T. W. G. L.; Van de Meerakker KGO; Steinbuch, M.; Veenhuizen, P. A. 2004. Simulation and control of slip in a continuously variable transmission, in *7th International Symposium on Advanced Vehicle Control: AVEC'04*, 23–27 August 2004, Arnhem, Netherlands, 111–115.

Bonsen, B.; Klaassen, T. W. G. L.; Pulles, R. J.; Simons, S. W. H.; Steinbuch, M.; Veenhuizen, P. A. 2005. Performance optimisation of the push-belt CVT by variator slip control, *International Journal of Vehicle Design* 39(3): 232–256. https://doi.org/10.1504/IJVD.2005.008473

Bulatov, V. P.; Krasny, V. A.; Schneider, Y. G. 1997. Basics of machining methods to yield wear- and fretting-resistive surfaces, having regular roughness patterns, *Wear* 208(1–2): 132–137. https://doi.org/10.1016/S0043-1648(96)07403-0

Costa, H. L.; Hutchings, I. M. 2015. Some innovative surface texturing techniques for tribological purposes, *Proceedings of the Institution of Mechanical Engineers, Part J: Journal of Engineering Tribology* 229(4): 429–448. https://doi.org/10.1177/1350650114539936

Dzyura, V.; Maruschak, P. 2021. *Tehnologichni metody zabezpechennja parametriv jakosti poverhon' til obertannja ta i'h profilometrychnyj kontrol'*. Ternopil', Ukrai'na. 170 s. (in Ukrainian).

Dzyura, V.; Maruschak, P.; Prentkovskis, O. 2021a. Determining optimal parameters of regular microrelief formed on the end surfaces of rotary bodies, *Algorithms* 14(2): 46. https://doi.org/10.3390/a14020046

Dzyura, V.; Maruschak, P.; Slavov, S.; Dimitrov, D.; Vasileva, D. 2021b. Experimental research of partial regular microreliefs formed on rotary body face surfaces, *Aviation* 25(4): 268–277. https://doi.org/10.3846/aviation.2021.15889

Dzyura, V.; Maruschak, P.; Slavov, S.; Gurey, V.; Prentkovskis, O. 2021c. Evaluating service characteristics of working surfaces of car parts by microgeometric quality parameters, *Machines* 9(12): 366. https://doi.org/10.3390/machines9120366

GOST R ISO 4287-2014. *Geometricheskie harakteristiki izdelij (GPS). Struktura poverhnosti. Profil'nyj metod. Terminy, opredelenija i parametry struktury poverhnosti.* (in Russian).

Guzanová, A.; Brezinová, J.; Bronček, J.; Maruschak, P.; Landová, M. 2015. Study of selected properties of coatings devoted to extreme tribo-corrosive conditions, *Materials Science Forum* 818: 32–36. https://doi.org/10.4028/www.scientific.net/MSF.818.32

Helsgaun, K. 2000. An effective implementation of the Lin–Kernighan traveling salesman heuristic, *European Journal of Operational Research* 126(1): 106–130. https://doi.org/10.1016/S0377-2217(99)00284-2

Kiselev, M. G.; Korzun, P. O.; Pavich, T. P. 2009. Opredelenie vida mikrorel'efa obrabotannoj poverhnosti, obespechivajushhego ee naibol'shuju ploshhad' i ob'em pri kontaktirovanii s zhidkost'ju, *Vestnik GGTU im. P. O. Suhogo* 4: 40–52. (in Russian).

Nagît, G.; Slătineanu, L.; Dodun, O.; Rîpanu, M. I.; Mihalache, A. M. 2019. Surface layer microhardness and roughness after applying a vibroburnishing process, *Journal of Materials Research and Technology* 8(5): 4333–4346. https://doi.org/10.1016/j.jmrt.2019.07.044

Nagorkin, M. N.; Fyodorov, V. P.; Kovalyova, E. V. 2018. Modeling of process of forming quality parameters for surfaces of parts by diamond burnishing taking into account technological heredity, *IOP Conference Series: Materials Science and Engineering* 327(4): 042071. https://doi.org/10.1088/1757-899X/327/4/042071

Nagorkin, M. N.; Fyodorov, V. P.; Nagorkina, V. V. 2017. Simulation modelling of tribotechnologies system and its parametric reliability assessment on tribotechnical parameters of the joints of sliding friction, *IOP Conference Series: Materials Science and Engineering* 177: 012079. https://doi.org/10.1088/1757-899X/177/1/012079

Nanbu, T.; Ren, N.; Yasuda, Y.; Zhu, D.; Wang, Q. J. 2008. Micro-textures in concentrated conformal-contact lubrication: effects of texture bottom shape and surface relative motion, *Tribology Letters* 29(3): 241–252. https://doi.org/10.1007/s11249-008-9302-9

Pawlus, P.; Reizer, R.; Wieczorowski, M. 2019. Reverse problem in surface texture analysis—one-process profile modeling on the basis of measured two-process profile after machining or wear, *Materials* 12(24): 4169. https://doi.org/10.3390/ma12244169

Sánchez Egea, A. J.; Rodríguez, A.; Celentano, D.; Calleja, A.; López de Lacalle, L. N. 2019. Joining metrics enhancement when combining FSW and ball-burnishing in a 2050 aluminium alloy, *Surface and Coatings Technology* 367: 327–335. https://doi.org/10.1016/j.surfcoat.2019.04.010

Seigars, C. M. 2016. *Modeling of a Continuously Variable Transmission and Clutching of a Snowmobile*. Honors Thesis. University of Maine, Orono, ME, US. 91 p. Available from Internet: https://digitalcommons.library.umaine.edu/honors/243/

Shnejder, Y. G.; Lebedinskij, G. G. 1970. Issledovanie vlijanija maslojomkosti rabochih poverhnostej gil'z cilindrov avtomobil'nyh dvigatelej na ih prirabatyvaemost', in *Uprochnjajushhe-kalibrujushhie i formoobrazujushhie metody obrabotki detalej: tezisy nauchno-prakticheskoj konferencii*, 13–15 nojabrja 1970 g., Rostov-na-Donu, SSSR, 92–93. (in Russian).

Slavov, S. D.; Dimitrov, D. M. 2018. A study for determining the most significant parameters of the ball-burnishing process over some roughness parameters of planar surfaces carried out on CNC milling machine, *MATEC Web of Conferences* 178: 02005. https://doi.org/10.1051/matecconf/201817802005

Slavov, S.; Iliev, I. 2016. Design and FEM static analysis of an instrument for surface plastic deformation of non-planar functional surfaces of machine parts, *Fiabilitate şi Durabilitate* 2: 3–9.

Swirad, S.; Pawlus, P. 2021. The effect of ball burnishing on dry fretting, *Materials* 14(22): 7073. https://doi.org/10.3390/ma14227073

Van der Meulen, S. 2010. *High-Performance Control of Continuously Variable Transmissions*. PhD Thesis. Eindhoven University of Technology, Netherlands. 261 p. https://doi.org/10.6100/IR692236

Volchok, A.; Halperin, G.; Etsion, I. 2002. The effect of surface regular microtopography on fretting fatigue life, *Wear* 253(3–4): 509–515. https://doi.org/10.1016/S0043-1648(02)00148-5

Wang, Z. W.; Chen, M. W.; Wu, J. W.; Zheng, H. H.; Zheng, X. F. 2010. A review of surface texture of tribological interfaces, *Applied Mechanics and Materials* 37–38: 41–45. https://doi.org/10.4028/www.scientific.net/AMM.37-38.41

Wos, S.; Koszela, W.; Pawlus, P. 2020. Comparing tribological effects of various chevron-based surface textures under lubricated unidirectional sliding, *Tribology International* 146: 106205. https://doi.org/10.1016/j.triboint.2020.106205

Yagyaev, E.; Shron, L.; Meniuk, D. 2020. Increasing the operational reliability of car variators due to creating regular surface microrelief by laser ablation, *IOP Conference Series: Materials Science and Engineering*: 012007. https://doi.org/10.1088/1757-899X/889/1/012007

Zajdes, S. A.; Hin, N. W. 2017. Vlijanie parametrov oscillirujushhego vyglazhivanija na sherohovatost' uprochnennyh poverhnostej, *Vestnik Irkutskogo gosudarstvennogo tehnicheskogo universiteta* 21(4): 22–29. https://doi.org/10.21285/1814-3520-2017-4-22-29 (in Russian).